

RESEARCH ARTICLE

“Medicinal Plant *Ananas comosus* Peel Extract Mediated Synthesis Cobalt Oxide Nanoparticle: Investigation of their Antioxidant and Antifungal Activity”

Terfo Yilma^{1,2,*} and Mikyas Kassaw¹

¹Applied Chemistry Department, School of Applied Natural Sciences, Adama Science and Technology University, Adama, P.O. Box. 1888, Ethiopia;

²Institute of Pharmaceutical Sciences, Adama Science and Technology University, Adama, Ethiopia.

***Corresponding author:** Terfo Yilma, Applied Chemistry Department, School of Applied Natural Sciences, Adama Science and Technology University, Adama, P.O. Box. 1888, Ethiopia, Tel: 0976760242, Email: peteryilma113@gmail.com.

Citation: Terfo Yilma, Mikyas Kassaw (2023) “Medicinal Plant *Ananas comosus* Peel Extract Mediated Synthesis Cobalt Oxide Nanoparticle: Investigation of their Antioxidant and Antifungal Activity”. *J Med Chem Drug Design* 1: 104

Abstract

Nanotechnology is the current hot area of finding drugs at nano levels to fight fungal infection and disease associated to free radicals. The *Ananas comosus* fruit peel is one medicinal plant that consist secondary metabolite used for capping and stabilizing agent for synthesized cobalt oxide nanoparticles (Co_3O_4 NPs). In this study we synthesized Co_3O_4 NPs using cobalt nitrate hexahydrate and *Ananas comosus* fruit peel extract and characterized using XRD, UV-DRS, SEM-EDX, and FTIR and evaluate antifungal and antioxidant activity. The result of this study showing that Co_3O_4 NPs revealed the average crystallite size of synthesized Co_3O_4 NPs found to be 12.58, 13.40, and 22.05 nm for the volume ratio of 1:1, 1:2, and 2:1, respectively. The energy band gap was found 3.33, 2.95, and 2.70 eV for the volume ratios above. The infrared analysis that confirms the phytochemical compound and Co^{2+} -O stretching found in Co_3O_4 NPs. The synthesized Co_3O_4 nanoparticles were good DPPH scavenger comparable to ascorbic acid and have antifungal properties against *C. albicans* and *A. niger* with inhibition zone increase from 7.12 to 14.5 mm and 8.5 to 16.10 mm respectively. The present work gives good starting up to find antifungal and antioxidant product for future.

Keyword: *Ananas comosus*; Cobalt oxide nanoparticle; characterization; Antioxidant; Antifungal.

Introduction

The interest in the science of nanotechnology in the application development of nanoparticles (NPs), which have a great impact on the development of different fields such as pharmaceuticals, cosmetics biomedical tools, food industry, agriculture, and engineering [1, 2]. The significant unique physicochemical properties of NPs differ significantly from their main counterpart. These properties are based on NPs a high large proportion of surface atoms, energy, and minimized imperfection [3]. Due to their surface plasmon light scattering, scale, shape, and surface, NPs outperform bulk materials. The chemical composition and mono-dispersity are very important in the modulation of their properties in different nano applications [4].

Chemically synthesizing NPs can contribute to the emergence of toxic substances that remain adsorbed on their surface and can affect human health in different biomedical applications [5]. Plants, natural polymers, and fungus have lately been used to create bio-inspired nanoparticles (NPs), and these NPs have gained enormous popularity due to their highly desirable physical, chemical, electrical, optical, nanoscale, low cost, and deep penetration features [6]. Plants extract is one of the important biological sources being contained in the phyto compounds that reduces the metal salt, after which aggregation and protection occur for the development of stable NPs [7, 6].

Medicinal plants have played a pivotal role in primary health care and offer a rich source of novel bioactive compounds in drug discovery and development [8]. Traditional medicine appears to be the source of healthcare particularly in the rural majority communities of Africa due to its intrinsic qualities, unique and holistic approaches, and its accessibility and affordability [8, 9].

Ethiopia is one of the six centers of biodiversity in the world with 6,500 species of higher plants where traditional medicine plays a significant role and vast majority of population lives in rural areas with little access to health services [6]. In recent years numerous Ethiopian medicinal plants have been validated in a scientific empirical framework through phytochemical analysis and subsequent bioassays [6]. The medicinal plants species are used to treat many diseases in Ethiopia [10]. Recently, more focusing on the green synthesis of metals and metals oxides NPs which aid in the development of nanomedicine applications such as specific delivery vehicles and medical treatment for associated chronic diseases [11].

Co₃O₄ NPs has attracted a lot of attention in the scientific community due to its ecological nature, ease of use, low cost, and strong electrical potential, and wide applications such as gas sensors, supercapacitors, heterogeneous catalysis, magnetic semiconductors, and field emission materials and medical application [12, 11]. Also, Co₃O₄ NPs are suitable for use in electronic devices and superconducting materials because having corrosion and oxidation resistance [13]. Co₃O₄ NPs have been used in cancer diagnosis, vaccination, and radiotherapy. Furthermore, it plays an important role as a cofactor of vitamin B12 and is effectively used for the detection of amino acids, glucose, and methanol [14].

The global NPs market is expected to reach 10,000 tons by 2026, with revenues of \$ 50 billion [1]. Numerous Physico-chemical processes of Co₃O₄ NPs formation have been discovered [15]. However, as mentioned above these methods have some limitations, such as it is long term, energy-intensive, non-ecological, non-scalable, and expensive. To avoid problems of lack of energy and toxicity to the environment, plant extracts, marines, wastes as well as the techniques of green approach are the best possible solution [16]. The primary source exploited in current research approaches for the creation of nanoparticles is the marine flora. Nanomedicine can transform discrete therapy into a worldwide disease treatment in the classification of animals. From a biological point of view, algae are one of the large classes of marine environmental systems. They have nutraceuticals proteins and a large number of secondary metabolites which improve their pharmaceutical properties [5]. The red algae have antioxidant activity [17, 18].

Besides, other species have anti-inflammatory and anticancer properties [18]. Furthermore, red algae have a lot of functional groups that able to be working as stabilizing, reducing, and capping agents during the synthesis of metallic and metal oxide nanoparticles. As to our knowledge this study is the first source of information on Co₃O₄ NPs biosynthesis using ananas cosmosus peel extract. Pineapple (*Ananas comosus*) is a perennial herb in the botanical family Bromeliaceae [19]. Pineapple has been proven to have various health benefits including anti-inflammatory, antioxidant activity, monitoring nervous system function, and healing bowel movement [20].

It is native to South America where the original seed species (wild) are still grown. Currently in Ethiopia the crop cultivated by small scale farming mainly in South and South-Western parts of the country [19]. Pineapple contains considerable amounts of bioactive compounds, dietary fiber, minerals, and nutrients that offer a number of health benefits and used as reduce or capping agent for synthesis of nanoparticles [20].

Biogenic Co_3O_4 NPs indicated DPPH free radical scavenging potential using phosphomolybdc based method while moderate antioxidant capacity and reducing power was demonstrated. Highest DPPH radical scavenging (57 %) was observed at 200 $\mu\text{g}/\text{ml}$ while the scavenging ability decreased at lower concentrations [21]. The antioxidant activity of *P. nigrum* mediated Co_3O_4 NPs was performed then reduced the toxic effect of ABTS free radicals and the antioxidant activity of Co_3O_4 NPs uncalcined at 100 °C was significantly high than those calcined at high temperature due there small size [22].

Oxidative stress was among the key factors of many disorders which an antioxidant compound can avoid. Moreover, the study of metal oxide nanoparticle's antioxidant activity has been among the main basic studies in nanoscience [1]. Also, anti-cancer nanotechnology focuses on the development of applications, especially cellular and molecular diagnoses, and treatment for cancer. Furthermore, the stability, drug encapsulation, specificity, and biocompatibility of nanomaterials make it have anticancer activity [23].

A recent study showed that magnetic Co_3O_4 NPs have fast cellular uptake properties that represent the most cause for success in medical biotechnology and have anti-cancer properties. An increase in the anticoagulant activity of heparin has been reported in conjunction with Au NPs biosynthesized using the extract from the earthworm [24]. In this study, green Co_3O_4 NPs synthesis was performed using *ananas cosmosus* peel extracts and screening *in vitro* antifungal and antioxidant activity. This metal oxide nanoparticle has been widely characterized by various methods including; UV, SEM, EDX, FTIR, and XRD.

Materials and Methods

Chemicals and Reagents

The chemicals, reagents and solvents used for this study were extra pure which cannot need extra purification techniques. These chemicals include sodium hydroxide (NaOH, 98 %), hydrochloric acid, ethanol (97 %), sulphuric acid (H_2SO_4 , 98 %), cobalt nitrate hexahydrate $\text{Co}(\text{NO}_3)_2 \cdot 6\text{H}_2\text{O}$ precursor salt, acetone, nutrient agar, potassium dichromate ($\text{K}_2\text{Cr}_2\text{O}_7$), 1,5-diphenylcarbazide, distilled water, ferric chloride (FeCl_3 , 99%) and chloroform (99.9%) etc.

Apparatuses and instruments used for this work were conical flask of different size (500, 100 mL), beaker (1000, 800, 500 and 100 mL), graduated cylinder (100, 50mL) volumetric flask (500, 100mL), measuring cylinder (100,50, 10mL), Whatman filter paper no 1 (120 cm, 90 cm diameter), magnetic stir, test tube, ceramic crucible, glass rod, spatula, pipette, thermometer, pH meter, centrifuge, mortar, and aluminum foils. oven, shaker (SK 300). The instruments used in this study were UV-Vis Diffraction reflectance spectroscopy, X-ray Diffractometer (Model XRD-7000, Japan), and Scanning electron microscope (SEM), Energy-Dispersive X-ray spectroscopy (EDX), and Fourier transfer infrared spectroscopy (FT-IR Perkin Elmer).

Collection of Ananas Cosmosus Fruit Peel

Ananas cosmosus fruit peel was collected from the local market in Adama, Ethiopia. The fruit samples were collected and washed with distilled water several times to remove extraneous matter or contaminants on the fruit peel. Then the washed plant peel was allowed to dry under shade at temperature to remove residual moisture content and make it ready for grinding. After drying, the peel was crushed using electrical grinding to produce a fine powder. Then the powder was packed within a plastic bottle followed by covering the whole body of the plastic bottle with aluminum foil.

Extract preparation

Extraction of the peel was done using 30 g of peel powder followed by adding 450 mL of distilled water and keeping two components on a hot plate. The mixed components were heated at 60 °C for 90 min until the required suspension was formed. Then, the extracted suspension was allowed cool at room temperature followed by filtration. Then the filtrates were kept in a

refrigerator at 4 °C for further work. The extract filtrate was used as a reducing and capping agent for the green synthesis of Co₃O₄ nanoparticles [25].

Preliminary Phytochemical Screening of *Ananas Comosus* Fruit Peel

The presence of phytochemicals like alkaloids, flavonoids, saponins, tannins, polyphenol, phenol, terpenoids, and reducing sugar in the aqueous extract of *ananas comosus* fruit peel was evaluated using standard methods [26].

Test for flavonoids: 0.5 mg portion of plant extract was dissolved in 15 mL of 96% ethanol and filtered. Then 3 mL of the filtrate were in a test tube, and 1 mL of potassium hydroxide solution was added. A dark yellow color indicated the presence of flavonoid compounds [27].

Test for saponins: To 0.5 mg of plant extract mixed with 5 mL of distilled water was added and shaken while heating to boil. The formation of foam to a length of 1 cm indicated the presence of saponins and steroids [28].

Test for phenols and tannins: The presence of phenolics and tannins from plant extract was screened according to the following methods with slight modification.

Sodium hydroxide test: Five mg of extract was dissolved in 0.5 mL of 20 % sulfuric acid solution. Followed by the addition of a few drops of aqueous sodium hydroxide solution, it turns blue which indicates the presence of phenols [28].

Ferric chloride test: To the plant extract 0.5 mL of 5% ferric chloride was added. The development of dark bluish-black color indicates the presence of tannins [28].

Test for terpenoids (Salkowski test): To 0.5 mg of plant extract was added 2 mL of chloroform Concentrated H₂SO₄ (3 ml) was carefully added to form a layer. The interface's reddish-brown coloring denotes the presence of terpenoids [29].

Test for steroids: Steroids were conducted following the methods of Anandharaj *et al.* (2021), one mg of the extracts was dissolved in 10 mL of chloroform and an equal volume of conc. H₂SO₄ was added to the sides of the test tube. The upper layer turns red and the H₂SO₄ layer showed yellow with green fluorescence which indicates the presence of steroids [30].

Detection of phytosterols (Salkowski test): The 0.5 mg of plant extract was treated with a few drops of chloroform and filtered. To the filtrate, a few drops of concentrated H₂SO₄ was added, shaken, and allowed to stand for a few min. The appearance of the golden yellow color indicates the presence of triterpenes [29].

Test for cardiac glycosides (Keller-Killiani test): 0.5 mg plant extract was diluted to 5 ml of water then 2 ml of dilute glacial acetic acid containing one drop of ferric chloride solution was added. Then 1 mL of concentrated sulfuric acid was added. A brown ring at the interface indicated the presence of a deoxy sugar characteristic of cardenolides. In the acetic acid layer, a greenish ring may form slightly above the brown ring and eventually expand across this layer, while a violet ring may occur below the brown ring [29].

Test for Alkaloid: The 0.5 mg of plant was stirred with 1 % HCl (0.5 mL) in a water bath for 5 min and filtered. The filtrates have been divided into three equal parts. To one portion of filtrate Wagner's reagent (Iodine in Potassium iodide solution) (1 mL) was added. The formation of an orange-colored precipitate indicates the presence of alkaloids [31].

Test for reducing sugars (Fehling's test): The aqueous ethanol extract (0.5 mg in 5 mL of water) was added to boiling Fehling's solution (A and B) in a test tube. The solution was observed for a color reaction [27].

Test for anthraquinones: The 0.5 mg of the extract is boiled with 10 mL of sulfuric acid (H_2SO_4) and filtered while hot. The filtrate was shaken with 5 mL of chloroform. The chloroform layer is pipetted into another test tube and 1 mL of dilute ammonia is added. The resulting solution is observed for color changes [29].

Synthesis of Cobalt Oxide Nanoparticles

Cobalt nitrate hexahydrate ($Co(NO_3)_2 \cdot 6H_2O$) and *ananas comosus* fruit peel was used for the synthesis of Co_3O_4 nanoparticles. To obtain ultra-fine nanoparticles of Co_3O_4 , optimizations were performed and the well-reduced Co_3O_4 nano size was taken for further characterizations and applications. In synthesis, $Co(NO_3)_2 \cdot 6H_2O$ was prepared and mixed within a reaction Erlenmeyer flask with peel extract approximately in (70:70), (33.33:66.66), and (66.66:33.3) means 1:1, 1:2 and 2:1 volume ratio. A small-sized magnetic bar was put inside the Erlenmeyer flask containing the extract and the precursor solution to enhance the reaction kinetics. The two components were stirred for 5:00 hrs at room temperature without applying any heat energy. After stirring time was completed, the pH of the formed suspensions was checked and controlled by adding some quantities of NaOH solution to facilitate precipitation. Then, the resulting suspension was stirred again for 30 min to maintain the uniform distribution of the added base. The formed suspension was placed in refrigerator overnight to enhance the precipitate formation and then after the supernatant was decanted carefully followed by centrifugation at 2000 rpm for 15 min followed by washing a minimum of three times using ethanol and distilled water. Then, it was collected using a ceramic crucible dish followed by placing it into a drying oven for 3 hrs at $100^\circ C$ and allowed to cool. The synthesized NPs was calcinated at $50^\circ C$ for 5 hrs by muffle furnace [43].

Finally, the nanoparticles were ground and ready for further characterizations and analysis (Figure 1).



Figure 1: Diagrammatic representation of synthesized cobalt oxide nanoparticles

Characterization of synthesized nanoparticles

The biosynthesized cobalt oxide nanoparticles were characterized using thermogravimetric analysis, X-ray diffraction, Energy Dispersive X-Ray Spectroscopy (EDS) Analysis scanning electron microscopy, ultraviolet-visible diffuse reflectance spectroscopy, and Fourier transform infrared spectroscopy. Furthermore, this study also evaluated the antifungal and antioxidant activity of the synthesized Cobalt Oxide nanoparticles against clinical pathogen by the disc diffusion method and DPPH assay.

Antifungal activities test

The anti-fungal activity was conducted against two common human pathogenic fungal strains *Candida albicans* (ATCC 26555) and *Aspergillus niger* (ATCC 10864) which were incubated on Potato dextrose agar (PDA) for three days at $30^\circ C$ [32, 33]. The anti-fungal activity was carried out by Kirby Bauer Disc diffusion technique against fungal strains [34]. Agar well diffusion test method is used to determine whether a fungal strain is resistant or susceptible to the synthesized NPs. This method was selected due to its simplicity, capacity to analyze multiple samples simultaneously, and its ability to work well with defined inhibitors [35].

The medium was prepared using potato dextrose agar (PDA). The autoclaved medium was poured into sterile plates (35-40

mL/plate) and the plates were allowed to solidify under the sterile condition at room temperature. After solidification, the plates were seeded with overnight grown culture approximately 1.5×10^5 CFU/mL by swabbing evenly onto the surface of the medium with a sterile cotton swab. *Fluconazole* was used as the standard drug used as positive control while DMSO was used as a negative control. The two fungal strains were tested with (50, 75, 100 $\mu\text{g/ml}$) using the paper disc-diffusion method [34] with slight modification.

For each concentration, 6 mm diameter Whatman.No1 filter paper discs were soaked with 100 μL solution of the above concentration for each sample and then these saturated paper discs were inoculated at the center of each petri dish having a fungal lawn with the help of sterile Cork borer [36]. The plates were incubated at 30 $^\circ\text{C}$ for 3 days, and the inhibition zone that appeared around the paper disc in each plate was determined by measuring the diameter of the inhibition.

Antioxidant Investigation test

Evaluation of the DPPH radical scavenging assay (RSA)

In terms of variables promoting health protection, antioxidants are crucial. Scientific evidence suggests that antioxidants reduce the risk for chronic diseases including cancer and heart disease [37]. The DPPH assay was used to assess the free radical scavenging activity of synthesized nano particles with different ratios. With this method the radical scavenging power of an antioxidant NPs was measured with the principle of a decrease in absorbance due to the donation of hydrogen from the sample to DPPH radical to produce stable DPPH-H and the color change from purple to yellow was observed (Figure 2).

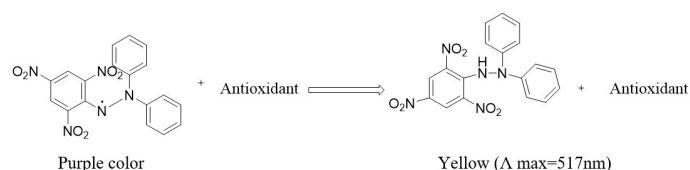


Figure 2: The structure of the DPPH radical and the scavenged radical.

The radical-scavenging activities of the NPs were determined using the DPPH method [38]. In the process, the samples were dissolved in methanol to afford 1 mg/mL. It was serially diluted in methanol to give a concentration of 500, 250, 125, and 62.5 $\mu\text{g/mL}$. To 1 mL of each concentration, 4 mL DPPH (0.04 % DPPH in MeOH) was added to make 100, 50, 25, and 12.5 $\mu\text{g/mL}$ solutions. Then all the samples prepared were incubated in an oven at 37 $^\circ\text{C}$ for 30 min and then absorbance was recorded at 517 nm using a UV-Vis spectrophotometer (Jenway 6858, England). A reaction solution without DPPH was used as blank and DPPH solution as a control and ascorbic acid as standard. The percentage inhibition was calculated using the formula (1)

$$\% \text{ Inhibition (RSA)} = \frac{[A \text{ control} - A \text{ test}]}{A \text{ control}} \times 100 \quad (1)$$

The DPPH radical scavenging activity of the samples is also expressed as IC_{50} , the concentration of the test compound to give a 50 % decrease of the absorbance from that of the control solution [37]. The IC_{50} values were calculated from the graph plotted from concentration versus % RSA determined using excel and interpreted as the smallest IC_{50} values mean the strongest radical scavenging concentration of extracts [2].

Results and Discussion

X-Ray diffractometer (XRD) Analysis of Calcinated Co₃O₄ NPs

The XRD pattern of Co₃O₄ NPs (Figure 3), shows using three volume ratios. The XRD of Co₃O₄ (1:1) NPs showed peaks appeared at 2θ values of ≈18.97°, 31.42°, 36.81°, 38.98°, 44.61°, 59.60°, 65.30°, and 76.10°. The XRD of Co₃O₄ (1:2) NPs showed peaks appeared at 2θ values of ≈ 18.91, 31.48, 36.86, 38.7, 44.92, 55.52, 59.2, and 77.7°, also the XRD of Co₃O₄ (2:1) NPs showed peaks appeared at 2θ values of ≈ 19.06, 31.49, 37.01, 42.37, 55.95, 59.33, 65.42 and 77.43° corresponding to the Miller indices value of (111), (220), (311), (222), (400), (422), (511), and (440), respectively. The diffraction peaks of Co₃O₄ NPs were found to be in good agreement with (JCPDS card No. 042-1467), which confirms the purity of the green synthesized Co₃O₄ NPs without the formation of any secondary phases and the result found to be in good agreement with the previously reported work [39]. According to Scherer's equation (2), the calculated average crystallite size of synthesized Co₃O₄ NPs was found to be 12.58, 13.40, and 22.05 nm for the volume ratio of 1:1, 1:2, and 2:1, respectively, and the result is presented in Table 1.

$$D = \frac{K\lambda}{\beta \cos\theta} \quad (2)$$

Where D is the average crystalline diameter K is the Scherer's constant (0.94), λ (0.15406 nm) is the X-ray wavelength, β is the full-width half maximum (FWHM) of the peak in radians, and θ is the Bragg's angle in degree. Among the three-volume ratio of Co₃O₄ NPs, (1:1) ratio has a better and smaller crystalline size than other counterparts. This might be contributed due to the presence of an equal volume of capping or reducing agent within salt precursor and more homogenization between the two components. Furthermore, the XRD spectra of Co₃O₄ (1:2) NPs possessed peak was sharp and high heights compared to the other counterparts and this indicates the material has more crystalline size nature. On the other hand, the XRD spectra of Co₃O₄ (2:1) NPs showed broad and short peak which indicate that the synthesized nanoparticles are less crystalline [17]. The average crystal size of the biosynthesized Co₃O₄ NPs has decreased when the ratio of the peel extract increased because the effective capping and stabilizing agent has able to hinder the aggregation. In this study, the volume of precursor salt increases to confirm the size enhancements of the NPs. The absence of additional peaks on the synthesized NPs indicated the degree of purity of the synthesized Co₃O₄ NPs [39, 40].

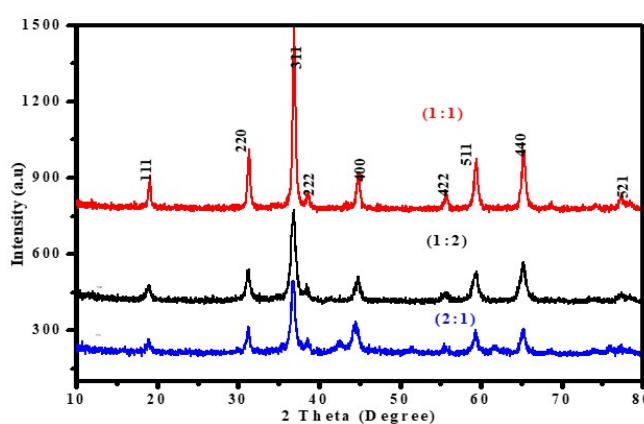


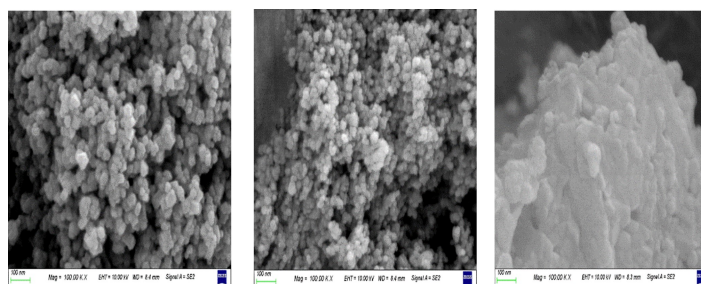
Figure 3: XRD pattern of *Ananas comosus* peel extract synthesized Co₃O₄ NPs.

Table 1: Calculated crystal size of synthesized Co_3O_4 NPs in three volume ratios

Ratios of Co_3O_4 NPs	2θ (degree)	FWHM (θ)	FWHM (3.14/180)	hkl	D(nm)	Average size(nm)
1:1	31.42	0.6879	0.012006	220	12.7131	12.58
	36.81	0.7600	0.013265	311	12.9587	
	59.60	0.7900	0.013788	511	12.0854	
1:2	31.48	0.6057	0.010571	220	14.4376	13.40
	38.70	0.8800	0.011053	311	10.1885	
	44.92	0.6333	0.015359	400	15.5507	
2:1	31.49	0.3880	0.006772	220	22.5455	22.05
	42.37	0.4629	0.006735	400	21.2853	
	37.01	0.3859	0.008079	311	22.3324	

Scanning Electron Microscopic (SEM) Analysis

Scanning electron microscope results confirmed the surface morphologies of biosynthesized Co_3O_4 NPs and the results are presented in **Figure 4 (a-c)**. The SEM image of Co_3O_4 NPs using 1:1 ratio by volume of the precursor and peel extract show in **Figure 4 (a)** was spherical shapes and is more deeply homogenized than the other counterpart of Co_3O_4 NPs. In addition to this, the morphology of Co_3O_4 NPs synthesized from 1:2 volume ratios of reactants in **Figure 4 (b)** showed predominantly spherical shape which might be due to the presence of more peel extract that stabilizes the formation of NPs and prevents their aggregation. The agglomeration of the particles is dependent upon the nature of compounds present in the extracts and attraction between the biomolecules and metal salts resulted in the aggregation of the NPs [40]. In the latter, the SEM image of Co_3O_4 NPs synthesized from 2:1 reactant ratio by volume in **Fig 4 (c)**, showed a honeycomb-like structure and more crystalline than the other ratio of Co_3O_4 NPs as the amount of the salt precursor was much greater than the amount of peel extract contains it and form aggregation. In the previous report, this aggregation or agglomeration may be caused due to polarity and electrostatic attraction between biomolecules and Co_3O_4 NPs [40].

Figure 4: The SEM Image of Co_3O_4 NPs a (1:1), b (1:2), and c (2:1) volume ratio.

Energy Dispersive X-Ray Spectroscopy (EDS) Analysis

The energy dispersive X-ray analysis of Co_3O_4 (1:1) NPs was shown in **Figure 5 (a-c)** and the sample obtained from SEM analysis in **Figure 5 (a)** with an equal volume ratio of salt precursor and peel extract. The EDS analysis of Co_3O_4 NPs was carried out using an internal standard at the energy of 0 up to 10 KeV. The EDS studies of results in **Figure 5 (b)** confirm that Co_3O_4 NPs contain Co and O as major elements. Moreover, the EDS analysis of Co_3O_4 NPs in **Figure(c)** showed two major peaks and other small peaks on the graph. The first strong peaks at 0.4 and 0.8 keV confirmed the presence of O and Co dominantly. The results indicate that the reaction product was composed of high purity Co_3O_4 NPs, and the composition obtained from EDS analysis of the normalized spectrum was Co (74.51%) and O (25.49 %) proving that the produced nanoparticle was the highest purified form. The EDS

analyses in this study showed similar results to the previous report [3]. The EDS also confirm additional minor peaks in trace amounts in Figure 5 (c) that might be due to the presence of other impurities like K and Zn, and Fe as contaminants from equipment and preparation of standards.

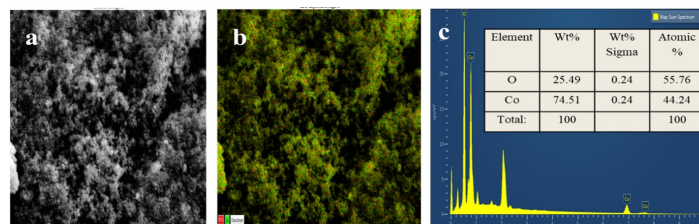


Figure 5: EDS image of Co_3O_4 (1:1) NP, a (SEM image of target sample), b (image of Co_3O_4 NP composition) c (EDS image Co_3O_4 NP).

Ultraviolet-visible Spectroscopy (UV-Vis DRS) Analysis

The energy band gap of synthesized Co_3O_4 NPs was estimated by using ultraviolet-visible diffuse reflectance spectroscopy as shown in **Figure 6 (a-b)**. Figure 6 (a), shows the reflectance spectra of synthesized Co_3O_4 NPs in different volume ratios characterized in the range of 200-800 nm. The peaks are assigned to the band gap of Co_3O_4 NPs owed to electron transitions from a lower energy state to a higher energy state. Here the Co ion is occupied in the distinct oxidation energy levels [41], so these ions perform as a P-type semiconductor, and its energy band gaps were evaluated from Tauc formula (3) and extrapolation procedure.

$$(\alpha h\nu) \frac{1}{n} = k(h\nu - E_g) \quad (3)$$

a

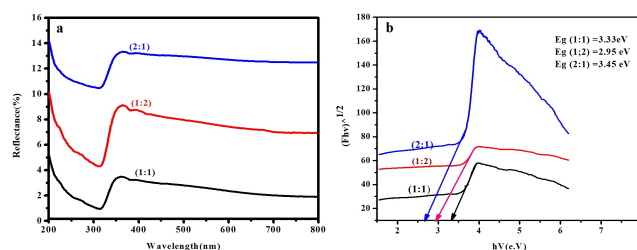


Figure 6 (a): UV-visible reflectance spectra and (b), band gap energy of Co_3O_4 NPs.

Fourier Transform Infrared (FTIR) Analysis

FTIR analysis **Figure 7 (a-c)**, shows the functional group of calcinated, and un-calcinated synthesized Co_3O_4 (1:1) NPs and the extracts of *Ananas comosus* peel powder which were recorded in the range of $4000\text{-}400\text{ cm}^{-1}$. The FT-IR spectra of *Ananas comosus* peel extract used for the synthesis of Co_3O_4 NPs were indicated in Figure 7 (a). The broad peak observed in peel extract of *Ananas comosus* around 3395 cm^{-1} spectrum represents the O-H stretching confirming aliphatic carboxylic acid. The prominent levels of absorption peak located at around 2921 cm^{-1} reveal the presence of sp^3 C-H stretching vibrations, of an aromatic aldehyde. The peak observed around $2360\text{-}2108\text{ cm}^{-1}$ represents the amide ($\text{C}=\text{N}$) functional groups. The $\text{C}=\text{O}$ stretching of the carbonyl functional group could be observed at 1717 cm^{-1} and the $\text{C}=\text{C}$ functional group for an extract of ananas peel powder at 1606 cm^{-1} . The C-O stretched functional group of the extract was located at 1242 cm^{-1} and the C-C functional group could be observed around 1029 cm^{-1} . Figure 7 (b) shows FTIR spectra of uncalcined Co_3O_4 NPs that exhibit the absorption peaks at 3365 cm^{-1} due to O-H stretching. The band at 1587 cm^{-1} due to $\text{C}=\text{C}$ stretching and the bands at 1354 cm^{-1} assigned to C-H stretching. The peaks

located at 1041cm^{-1} due to the presence of the C-C functional group. The band at 827cm^{-1} corresponds to the O-Co-O bridging vibration and at 560cm^{-1} the stretch of Co-O vibration [3]. Figure 7 (c) also, shown calcinated Co_3O_4 NPs at $500\text{ }^\circ\text{C}$ and have shown some peak on the graph at 1380 nm and 870 nm that might indicate the finger print region that shows metal and peel extract interaction and Co-O reaction during NPs formation. The vibration stretching band for the high annealed temperature was noticed around 650 and 547 cm^{-1} , which are assigned to the elongation of the $\text{Co}^{3+}\text{-O}$ bond and $\text{Co}^{2+}\text{-O}$ stretching, respectively.

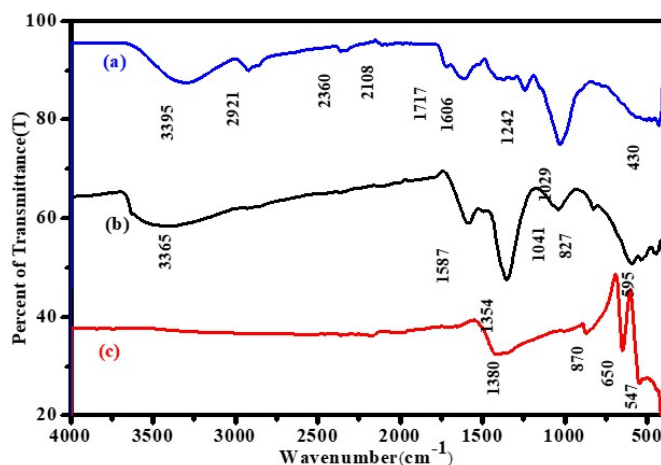


Figure 7 FTIR spectra of (a) *Ananas comosus* plant peel powder (b) Un calcinated synthesized of Co_3O_4 NPs and (c) calcinated synthesis of Co_3O_4 NPs.

Phytochemical Analysis of the Peel extract

The qualitative analysis of the bioactive compound present in the *Ananas comosus* peel extract has been analyzed and shows the presence of different phytochemicals which revealed it was the reservoirs of biologically active metabolites Table 2. The bioactive compounds such as reducing sugar, Alkaloid, phenol, Tannis, Flavonoids, Saponins, and Terpenoids in the peel extract were confirmed by different tests, and they are involved in their color changes. Based on the result the natural existence of phytochemicals in the peel extract was used as reducing and capping agents during the synthesis of Co_3O_4 NPs [6].

Table 2: Phytochemical screening of ananas comosus peel extract

No	Phytochemical constituent	Reagent added	Color observed	Results
1	Reducing sugar	Benedict test	Blue-green	+
2	Alkaloid	Wagner reagent	Reddish	+
3	Polyphenol	Ferric chloride	Dark green/ black	+
4	Flavonoids	Alkaline Reagent Test	Yellow	+
5	Tannins	Ferric chloride	Green	-
6	Saponins	Distilled water	Stable persistent	-
7	Terpenoids	Chloroform and H_2SO_4	Reddish brown	+

‘+’ indicates the presence and ‘-’ indicates the absence

Antifungal activity of biosynthesized Co_3O_4 NPs with different ratios

The synthesized Co_3O_4 NPs has moderate antifungal effects against selected fungal strains. The antifungal effects of the synthesized nanoparticles with different ratios shows different result against both strains in concentration dependent manner as depicted in Table 3. To compare the result 1:2 Co_3O_4 NPs has stronger inhibition zone against *A. niger* with inhibition zone of (16.10±0.45 mm) compared to positive standard *fluconazole* having an inhibition zone of (25±0.35 mm) against *A. niger* (Figure 8). The 2:1 Co_3O_4 NPs has comparable inhibition effect on both strains with inhibition zone of (14.7 ±0.24 mm) and (15±0.25 mm) against *C. albicans* and *A. niger* at 100 µg /ml concentration of sample respectively. The 1:1 Co_3O_4 NPs was exhibiting relatively smaller effects compared to the other two ratio which having inhibition zone of 11.7±0.25 mm and 13.85±0.42 mm at maximum concentration of sample. From the result we can suggest the antifungal effects of synthesized NPs was mainly emanated due to toxicity effects of cobalt metal to the fungal strains or the bioactive metabolites from plant extracts. The synthesized Co_3O_4 NPs in the current study have very small sizes, and, therefore, retains a high surface area to volume ratio possibly resulting in surfaces with high free energy content. Also, the efficient release of cobalt ions from the surface of Co_3O_4 NPs, and the production of free reactive oxygen species (ROS) could possibly be other factors that contributed to their enhanced antifungal activities.

There have been no studies thus far elucidating the mechanisms of the antifungal activities of Co_3O_4 NPs using *ananas cosmosus* fruit peel against filamentous fungi, although the present study strongly endorses their potential as antifungal agents. The fungal cell membrane contains ergosterol that acts as bio-regulator by maintaining its fluidity and, therefore, is responsible for maintaining the functionality that involves substance transport [42]. The high inhibitory activities of Co_3O_4 NPs could also possibly be accredited to the generated reactive oxygen species (ROS) causing lipid peroxidation, and the cobalt ions for their direct interaction with the fungal ribosomes and proteins, leading to their disassembly and inactivation [17].

Table 3: Zone of inhibition (mm) of Co_3O_4 NPs against *C. albicans* and *A. niger* fungal strains.

Samples ratio (salt: extracts)	Conc. (µg /ml)	Fungal strains and Zone of Inhibitions in mm	
		<i>C. albicans</i> (ATCC 26555)	<i>A. niger</i> (ATCC 10864)
1:1 Co_3O_4 NPs	1 (50 µg /ml)	7±1.12	8.5±0.56
	2 (75 µg /ml)	8.8±0.16	10.8±0.43
	3 (100 µg /ml)	11.7±0.25	13.85±0.42
1:2 Co_3O_4 NPs	1 (50 µg /ml)	12 ±0.67	11.7±0.25
	2 (75 µg /ml)	13.8±0.40	15.9±0.65
	3 (100 µg /ml)	14.5±0.30	16.10±0.45
2:1 Co_3O_4 NPs	1 (50 µg /ml)	9.4 ±0.00	11±0.51
	2 (75 µg /ml)	11±0.57	13.5±0.22
	3 (100 µg /ml)	14.7 ±0.24	15±0.25
Standard drug	<i>Fluconazole</i>	22.5±0.87	25±0.35

The experiments done three times and the result expressed as mean± standard deviation, where 1=50 µg /ml, 2=75 µg /ml, 3=100 µg /ml).

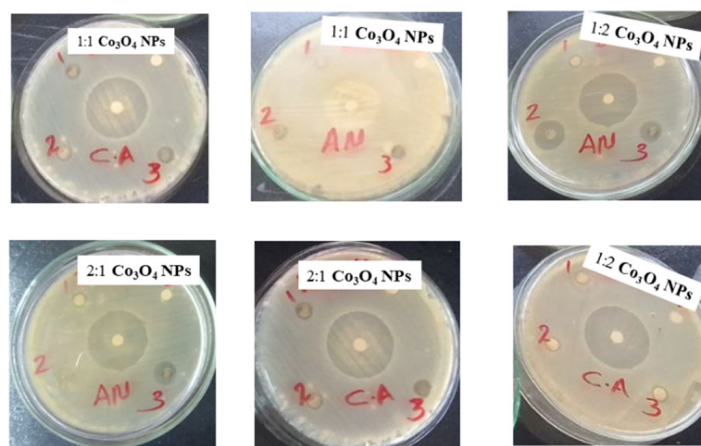


Figure 8: Disc diffusion antifungal activity evaluation of the synthesized Co_3O_4 NPs against *Aspergillus niger* (AN), and *Candida albicans* (CA).

Antioxidant activities of synthesized Co_3O_4 NPs

The radical scavenging activities of synthesized NPs using different ratios of plant extracts and salt concentration exhibited strong radicals scavenging properties with DPPH assay techniques used in this study. In all case the antiradical activities observed in concentration dependent manner to all ratios Table 4. To compare the result the ratio (1:2) Co_3O_4 NPs has very strong radical scavenging power compared to the other ratios of samples and it was very comparable to the standard ascorbic acid (AA) used with percentage of radical scavenging with 95.61 % at maximum concentration at 100 $\mu\text{g}/\text{mL}$ which was 98.7 % for AA (**Figure 9**). The second moderate radical snatching activities observed for the ratio 1:1 Co_3O_4 NPs which have percentage of activity 74.78 % at maximum concentration and this result almost moderate relative to ascorbic acid at this concentration. The low antiradical properties observed in the ratio of 1:2 Co_3O_4 NPs which was insignificant inhibition of free radicals compared to others and this might be due the sharp and having highest peaks compared to the other counterparts and this indicates the material has more crystalline size nature which have direct effect on reducing increased absorbance that decrease the scavenging power of free radicals. Generally, from the present result we can suggested that antiradical properties of cobalt oxide NPs can be either due to the polyphenol and flavonoids class in the plant extracts which also observed from the FTIR and qualitative phytochemical result or the anticancer nature of the metal as previously reported [1, 2].

Table 4: % Radical scavenging activity of synthesized Co_3O_4 NPs and the Ascorbic acid (AA).

Conc. ($\mu\text{g}/\text{mL}$)	Absorbance				DPPH % inhibition			
	1:1 Co_3O_4 NPs	1:2 Co_3O_4 NPs	2:1 Co_3O_4 NPs	AA	1:1 Co_3O_4 NPs	1:2 Co_3O_4 NPs	2:1 Co_3O_4 NPs	AA
12.5	0.28	0.72	0.23	0.03	69.29	21.04	74.78	96.71
25	0.27	0.69	0.16	0.02	70.39	24.31	82.45	97.81
50	0.25	0.65	0.06	0.014	72.58	24.33	93.42	98.50
100	0.23	0.57	0.04	0.012	74.78	37.49	95.61	98.70
Control 0.9118								

%RSA= Radical scavenging activity, and the results were expressed as mean \pm standard deviation

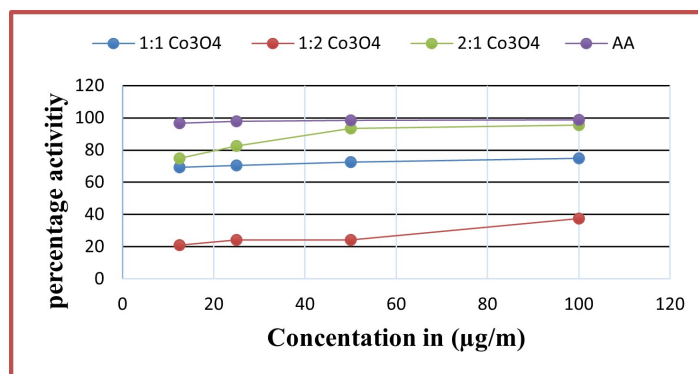


Figure 9: Radical scavenging activity (%) of Co₃O₄ NPs and the positive reference (Ascorbic acid).

Conclusion

Cobalt oxide nanoparticles (Co₃O₄ NPs) were fabricated using an eco-friendly method using *ananas comosus* peel extracts. The average crystallite size of synthesized Co₃O₄ NPs was found to be 12.58, 13.40, and 22.05 nm for the volume ratio of 1:1, 1:2, and 2:1, respectively. The anti-fungal activity of the Co₃O₄ NPs was investigated and exhibited that the inhibition zone was increased from 7.12 to 14.5 and from 8.5 to 16.10 mm against both *C. albicans* and *A. niger* with concentrations of nanoparticles grew from 50 µg/mL to 100 µg/mL, respectively. Furthermore, the antifungal activities of Co₃O₄ NPs were different for different ratio of sample and concentration for the two fungal strains. Moreover, the antioxidant activity was analyzed and revealed that the maximum radical scavenging of DPPH obtained 95.61 % at 100 µg/ml of Co₃O₄ NPs which was comparable to the positive reference at the same concentration. From the present study we can conclude that searching antifungal drug candidates was the future research endeavors. Not only this but also searching antioxidant materials using nanoscience from the *ananas comosus* and cobalt metal was the promising future solution for disease associated to reactive oxygen species (ROS) to overcome the current headache issue of synthetic antioxidant like butylated hydroxy toluene (BHT) and butylated hydroxy anisole (BHA). The researcher also strongly recommend further characterization techniques using modern instrument to full illustrate the antifungal and antioxidant properties cobalt oxide nanoparticles using this promising medicinal plant.

Acknowledgement

The authors acknowledge Adama Science and Technology University for research grant under Grant (ASTU/AS-R/003/2020).

Funding

This research was funded by the Researchers Supporting Project number ((ASTU/AS-R/003/2020), Adama science and technology university (ASTU), Adama, Ethiopia.

Compliance with Ethical Standards

Conflict of interest

All procedures in this study were per international ethical standards. The research involved no human participants and supplementary data was obtained upon request author.

References

1. JS Ajarem, SN Maooda, AA Allam, MM Taher, M Khalaf (2022) "Benign Synthesis of Cobalt Oxide Nanoparticles Containing Red Algae Extract: Antioxidant, Antimicrobial, Anticancer, and Anticoagulant Activity," *J. Clust. Sci* 33: 717-28.
2. LA Castro-Concha, J Tuyub-Che, A Moo-Mukul, FA Vazquez-Flota, ML Miranda-Ham (2014) "Antioxidant capacity and total phenolic content in fruit tissues from accessions of capsicum chinense Jacq. (Habanero Pepper) at different stages of ripening," *Sci. World J* 2014.
3. G Asha, V Rajeshwari, G Stephen, S Gurusamy, DC Jeniba (2021) "Materials Today: Proceedings Eco-friendly synthesis and characterization of cobalt oxide nanoparticles by sativum species and its photo-catalytic activity," *Mater. Today Proc* 1-8.
4. AS Rini, SD Rahayu, Y Hamzah, TM Linda, Y Rati (2021) "Effect of pH on the morphology and microstructure of ZnO synthesized using ananas comosus peel extract," *J. Phys. Conf. Ser* 2019: 1.
5. MG Demissie, FK Sabir, GD Edossa, BA Gonfa (2020) "Synthesis of Zinc Oxide Nanoparticles Using Leaf Extract of *Lippia adoensis* (Koseret) and Evaluation of Its Antibacterial Activity," *J. Chem* 2020.
6. T Desalegn, HCA Murthy, Y Adimasu (2021) "Medicinal Plant *Syzygium Guineense* (Willd .) DC Leaf Extract Mediated Green," 8: 1.
7. S Phongtongpasuk, S Kedpratum, N Yongvanich (2022) "Exposure of Ananas Comosus to Zinc Oxide Nano-Powder in Vitro: Physiology and Bromelain Production," *Suranaree J. Sci. Technol* 29: 6.
8. M Anza, et al. (2021) "Antimicrobial activity, in silico molecular docking, admet and dft analysis of secondary metabolites from roots of three ethiopian medicinal plants," *Adv. Appl. Bioinforma. Chem* 14: 117-32.
9. W Galma, M Endale, E Getaneh, R Eswaramoorthy, T Assefa (2021) "Antibacterial and antioxidant activities of extracts and isolated compounds from the roots extract of *Cucumis prophetarum* and in silico study on DNA gyrase and human," *BMC Chem* 1-17.
10. W Abebe (2016) "An Overview of Ethiopian Traditional Medicinal Plants Used for Cancer Treatment," 14: 1-16.
11. N Zahin, et al. (2020) "Nanoparticles and its biomedical applications in health and diseases: special focus on drug delivery," *Environ. Sci.Pollut. Res* 27: 19-68.
12. MS Chavali, MP Nikolova (2019) "Metal oxide nanoparticles and their applications in nanotechnology," *SN Appl. Sci* 1: 1-30.
13. N Mubraiz, A Bano, T Mahmood (2021) "Microbial and plant assisted synthesis of cobalt oxide nanoparticles and their antimicrobial activities," *Agronomy* 11: 1-20.
14. N Jalilian, GD Najafpour, M Khajouei (2019) "Enhanced Vitamin B12 Production using *Chlorella vulgaris*," *Int. J. Eng. Trans. A Basics* 32: 1-9.
15. AA Urabe, WJ Aziz (2019) "Biosynthesis of cobalt oxide (Co₃O₄) nanoparticles using plant extract of *Camellia sinensis* (L), *Kuntze* and *Apium graveolens* as the anti-bacterial application," 24: 357-65.
16. AT Khalil, et al. (2020) "Physical properties, biological applications and biocompatibility studies on biosynthesized single

- phase cobalt oxide (Co₃O₄) nanoparticles via *Sageretia thea* (Osbeck.),” *Arab. J. Chem* 13: 606-19.
17. M Hafeez, et al. (2020) “Green synthesis of cobalt oxide nanoparticles for potential biological applications,” *Mater. Res. Express* 7: 2.
18. JC Lee, et al. (2013) “Marine algal natural products with anti-oxidative, anti-inflammatory, and anti-cancer properties,” *Cancer Cell Int* 13: 1–7.
19. T Mulualem, N Semman, G Etana (2021) “Physico-chemical and Sensory Characterization of Pineapple (*Ananas comosus* (L) Varieties in Southwest Ethiopia Agrotechnology,” 6-11.
20. M Mohd, N Hashim, S Abd, O Lasekan (2020) “Pineapple (*Ananas comosus*): A comprehensive review of nutritional values, volatile compounds, health benefits, and potential food products,” *Food Res. Int* 137: 109675.
21. M Maaza, et al. (2021) “Physical properties, biological applications and biocompatibility studies on biosynthesized single phase cobalt oxide (Co₃O₄) nanoparticles via *Ananas comosus* (L),” *Arab. J. Chem* 14: 60-9.
22. S Haq, F Abbasi, M Ben Ali, A Hed, A Mezni, et al. (2021) “Green synthesis of cobalt oxide nanoparticles and the effect of annealing temperature on their physiochemical and biological properties, *Materials Research Express* 8: 1-11.
23. MH Teaima, MK Elasal, SA Omar, MA El-Nabarawi, KR Shoueir (2020) “Eco-friendly synthesis of functionalized chitosan-based nanoantibiotic system for potential delivery of linezolid as antimicrobial agents,” *Saudi Pharm* 28: 859-68.
24. HK Kim, et al. (2013) “Earthworm extracts utilized in the green synthesis of gold nanoparticles capable of reinforcing the anticoagulant activities of heparin,” *Nanoscale Res. Lett* 8: 1–7.
25. NOM Dewi, Y Yulizar, DO Bagus Apriandanu (2019) “Green synthesis of Co₃O₄ nanoparticles using *Euphorbia heterophylla* L. leaves extract: Characterization and photo catalytic activity,” *IOP Conf. Ser. Mater. Sci. Eng* 509: 0–7.
26. MS Auwal, S Saka, IA Mairiga, KA Sanda, A Shuaibu, et al. (2014) “Preliminary phytochemical and elemental analysis of aqueous and fractionated pod extracts of *Acacia nilotica* (Thorn mimosa).” *Vet. Res. forum an Int. Q. J* vol: 95-100.
27. S Chintalapani, MS Swathi, ML Narasu (2018) “Phytochemical screening and in vitro antioxidant activity of whole plant extracts of *sesuvium portulacastrum*” *Asian J. Pharm. Clin. Res* 11: 322-27.
28. TS Geetha, N. Geetha (2014) “Phytochemical screening, quantitative analysis of primary and secondary metabolites of *Cymbopogon citratus* (DC) stapf. Leaves from Kodaikanal hills, Tamilnadu,” *Int. J. PharmTech Res* 6: 521-29.
29. GA Ayoola, et al. (2008) “Method Spots Test,” *Trop. J. Pharm. Resear*, vol. 7: 1019-24.
30. B Anandharaj, M Sathya, M Maheshwari, B Priyadharshini, VP Arun, et al. (2021) “Preliminary Phytochemical Screening of Natural Anti-dandruff plant *Phyllanthus niruri* (L.) Greene (*Lippianodiflora*),” *Int. J. Res. Publ. Rev* 2: 1930-32.
31. S Dey, N Dey, AK Ghosh (2010) “Phytochemical Investigation and Chromatographic Evaluation of the Different Extracts of Tuber of *Amorphophallus paeoniifolius* (araceae),” *Int. J. Pharm. Biomed. Res.*, vol. 1: 150-57.
32. A Gizaw, et al. (2022) “Phytochemical Screening and In Vitro Antifungal Activity of Selected Medicinal Plants against *Candida albicans* and *Aspergillus niger* in West Shewa Zone, Ethiopia,” 2022: 1-8.

33. HNH Tran, L Graham, EC Adukwu (2020) "In vitro antifungal activity of Cinnamomum zeylanicum bark and leaf essential oils against *Candida albicans* and *Candida auris*," *Appl. Microbiol. Biotechnol.*, 104: 8911-24.
34. S Khalid, SA Majid, MA Akram (2019) "The prophylactic effect of *Ranunculus laetis* (Wall)-mediated silver nanoparticles against some Gram-positive and Gram-negative bacteria," *Bull. Natl. Res. Cent.*, vol. 43: 1.
35. A Manoharan, R Pai, V Shankar, K Thomas, MK Lalitha (2003) "Comparison of disc diffusion & E test methods with agar dilution for antimicrobial susceptibility testing of *Haemophilus influenzae*," *Indian J. Med. Res* 117: 81-7.
36. S Nazir, B Li, K Tahir, A Khan, Z Ul, et al. (2013) "Antimicrobial activity of five constituents isolated from *Ranunculus muricatus*," 7: 3438-43.
37. A Kalbessa, A Dekebo, H Tesso, T Abdo, N Abdissa, et al. (2019) "Chemical Constituents of Root Barks of *Gnidia involucrata* and Evaluation for Antibacterial and Antioxidant Activities," *J. Trop. Med* 2019: 1-10.
38. P Rajesh, P Natvar (2011) "In vitro antioxidant activity of coumarin compounds by DPPH, Super oxide and nitric oxide free radical scavenging methods," *J. Adv. Pharm. Educ. Res* 1: 52-68.
39. ET Bekele, et al. (2022) "Solanum tuberosum leaf extract Templated Synthesis of Co₃O₄ Nano particles for Electrochemical Sensor and Antibacterial Applications," 2: 1-16.
40. M Siddique, et al. (2021) "Green synthesis of cobalt oxide nanoparticles using *Citrus medica* leaves extract: characterization and photo-catalytic activity," 23: 663-81.
41. CT Anuradha, P Raji (2021) "Citrus limon fruit juice-assisted biomimetic synthesis, characterization and antimicrobial activity of cobalt oxide (Co₃O₄) nanoparticles," *Appl. Phys. A Mater. Sci. Process* 127: 1-9.
42. KG Akpomie, et al. (2021) "Ananas comosus peel-mediated green synthesized magnetite nano particles and their antifungal activity against four filamentous fungal strains" *Biomass Convers. Biorefinery*, 1-12.
43. M Salavati-Niasari, A Khansari, F Davar (2009) "Synthesis and characterization of cobalt oxide nanoparticles by thermal treatment process," *Inorganica Chim. Acta* 362: 4937-42.